



Grant Agreement No. 783169
U-Geohaz – “Geohazard impact
assessment for urban areas”

Deliverable D2.5: Updated Active deformation areas map (ADA)

**A deliverable of WP2: Tools to support the Early Warning for Landslides
geohazard**

Due date of deliverable: 30/06/2019
Actual submission date: 06/08/2019

Lead contractor for this deliverable: CTTC

Dissemination Level		
PU	Public	x
PP	Restricted to other programme participants (including the Commission Services)	
RE	Restricted to a group specified by the Consortium (including the Commission Services)	
CO	Confidential, only for members of the Consortium (including the Commission Services)	
TN	Technical Note, not a deliverable, only internal for members of the Consortium	



European Union
Civil Protection and
Humanitarian Aid

Table of Content

EXECUTIVE SUMMARY	3
REFERENCE DOCUMENTS	4
1 INTRODUCTION.....	6
2 DATASET DESCRIPTION	7
3 PROCEDURE DESCRIPTION	9
3.1 Deformation Activity Map.....	9
3.1.1 STEP-0 Calculation of interferograms and coherences	10
3.1.2 Coherence analysis.....	10
3.1.3 STEP-1 Linear velocity estimation	12
3.1.4 STEP-2 Residual interferograms	13
3.1.5 STEP-3 Time Series (TS) estimation	13
3.1.6 STEP-4 APS estimation and removal	13
3.1.7 STEP-5 Add linear component.....	15
3.1.8 STEP-6 Geocoding	15
3.2 Active Deformation Areas Map and DAM	15
4 MAP DESCRIPTION AND USE.....	16
4.1 DAM Time series.....	18
5 RESUMED OBSERVATIONS.....	18
5.1 Improvements	18
5.2 Map interpretation notes.....	18
6 REFERENCES.....	20

EXECUTIVE SUMMARY

This document contains a short description of the final Deformation Activity maps obtained over the Valle d'Aosta test site. These results have been obtained in the frame of the task "2.3 Landslide activity maps" of the work package 2 "Tools to support the Early Warning for Landslides geohazard" and represents the last version of the deliverable 2.5 "Updated Active deformation areas map (ADA)", led by CTTC. The main goal of WP1 is to implement and test a procedure to fully exploit the 6-day repeatability of the Sentinel-1 constellation, in order to continuously assess the potential impact of active landslides on urban areas and critical infrastructures.


REFERENCE DOCUMENTS

N°	Title
RD1	DoW Part B
RD2	D2.3.1
RD3	D13(V0)

CONTRIBUTORS

Contributor(s)	Company	Contributor(s)	Company
Anna Barra	CTTC	Enric Fernandez	CTTC
Oriol Monserrat	CTTC	Jose Navarro	CTTC
Michele Crosetto	CTTC		

REVIEW: CORE TEAM

Reviewed by	Company	Date	Signature
Oriol Monserrat	CTTC	09/07/2018	

1 INTRODUCTION

This document is a short report on the delivered deformation activity map and ADA map (version 1) of the Valle d'Aosta test site (Figure 1-1). The area of study is around 1800 km², it has been widened with respect to the first deliverable in order to totally include the Valpelline and Val di Grossoney valleys, areas of interest for some known gravitational movements.



Figure 1-1 Area of study: Valle d'Aosta (Italy).

The deformation activity map (DAM) is the first result of the Sentinel-1 (S-1) DInSAR processing; it consists in the estimated annual velocity and deformation time series (TS) in correspondence of selected points (PS). DAM is the input to generate the Active Deformation Areas Map, which is derived by a semi-automatic extraction of the most significant detected active deformation areas (ADA). In this step, we deliver the final version of the maps, with many improvements achieved with respect to the version zero.

Valle d'Aosta test site is characterized by highly variable topographic relief (ranging from 300 m a.s.l. to peaks higher than 4000 m a.s.l.) and steep slopes, which imply some spatial-sampling limitations due the SAR geometry of acquisition. The regional climate is characterized by wide range of temperatures and rainfall/snowfall, varying a lot from the mountainous zone to the bottom of the valleys. This climate variation is strongly reflected in the local radar response. The mayor constraining factor is the snow coverage, which strongly affects the coherence and the spatial sampling of the results. Valle d'Aosta land is mainly covered by forest, natural grassland, and rock outcrops with little or no vegetation, few urban areas are localized at the bottom of the valley, where the PS density increase with respect to the mountainous zones.

The described characteristics make the area a challenging zone from the radar point of view. A strong effort need to be done in order to overcome problems of low PS coverage, strong atmosphere component, and noisy results, including their reliability and interpretation.

This document consists of 5 sections: after the introduction, Section 2 describes the Sentinel-1 dataset at hand; Section 3 describes some aspects of the procedure; Section 4 the delivered map and finally Section 5 underline particular aspects about the results.

2 DATASET DESCRIPTION

The processed dataset consists of 153 Sentinel-1 (A and B) Wide Swath images acquired during the period spanning from January 2, 2015 (corresponding to the first available image over the study area) to September 25, 2018 (see Table 2-1 and Table 2-2). Table 2-1 shows the acquisition dates of the images. At the end of December 2016, when Sentinel-1B started the acquisitions over the study area, there is a change in the most frequent temporal baseline, passing from 12 days to 6 days. It can be observed that the maximum time interval of consecutive images is 36 days, which occur in one case, between the images 44 and 45. The main characteristics of the used images are summarized in Table 2-2. The processed datasets consist in 2 bursts x 2 swaths.

To remove the topographic contribution from the interferograms, we have used the 90 m resolution SRTM Digital Elevation Model provided by NASA, and the precise orbits provided by the European Space Agency (ESA).

Nº image	Date	Nº image	Date	Nº image	Date	Nº image	Date
1	02/01/2015	41	26/04/2016	81	21/05/2017	121	15/02/2018
2	14/01/2015	42	08/05/2016	82	27/05/2017	122	27/02/2018
3	26/01/2015	43	20/05/2016	83	02/06/2017	123	11/03/2018
4	07/02/2015	44	01/06/2016	84	08/06/2017	124	23/03/2018
5	19/02/2015	45	07/07/2016	85	20/06/2017	125	29/03/2018
6	03/03/2015	46	19/07/2016	86	26/06/2017	126	04/04/2018
7	15/03/2015	47	31/07/2016	87	02/07/2017	127	10/04/2018
8	27/03/2015	48	12/08/2016	88	14/07/2017	128	22/04/2018
9	08/04/2015	49	24/08/2016	89	20/07/2017	129	28/04/2018
10	20/04/2015	50	05/09/2016	90	26/07/2017	130	04/05/2018
11	02/05/2015	51	17/09/2016	91	01/08/2017	131	10/05/2018
12	14/05/2015	52	29/09/2016	92	07/08/2017	132	16/05/2018
13	26/05/2015	53	23/10/2016	93	13/08/2017	133	22/05/2018
14	07/06/2015	54	04/11/2016	94	19/08/2017	134	28/05/2018
15	19/06/2015	55	16/11/2016	95	25/08/2017	135	03/06/2018
16	01/07/2015	56	28/11/2016	96	06/09/2017	136	09/06/2018
17	13/07/2015	57	10/12/2016	97	12/09/2017	137	15/06/2018
18	25/07/2015	58	22/12/2016	98	18/09/2017	138	21/06/2018
19	06/08/2015	59	28/12/2016	99	24/09/2017	139	27/06/2018
20	18/08/2015	60	03/01/2017	100	30/09/2017	140	09/07/2018
21	30/08/2015	61	09/01/2017	101	06/10/2017	141	15/07/2018
22	11/09/2015	62	15/01/2017	102	12/10/2017	142	21/07/2018
23	23/09/2015	63	27/01/2017	103	18/10/2017	143	27/07/2018
24	05/10/2015	64	02/02/2017	104	24/10/2017	144	02/08/2018
25	17/10/2015	65	08/02/2017	105	30/10/2017	145	08/08/2018
26	29/10/2015	66	14/02/2017	106	05/11/2017	146	14/08/2018
27	10/11/2015	67	20/02/2017	107	17/11/2017	147	20/08/2018
28	22/11/2015	68	26/02/2017	108	23/11/2017	148	26/08/2018
29	04/12/2015	69	04/03/2017	109	29/11/2017	149	01/09/2018
30	16/12/2015	70	10/03/2017	110	05/12/2017	150	07/09/2018
31	28/12/2015	71	16/03/2017	111	11/12/2017	151	13/09/2018
32	09/01/2016	72	28/03/2017	112	17/12/2017	152	19/09/2018
33	21/01/2016	73	03/04/2017	113	23/12/2017	153	25/09/2018
34	02/02/2016	74	09/04/2017	114	29/12/2017		
35	14/02/2016	75	15/04/2017	115	04/01/2018		
36	26/02/2016	76	21/04/2017	116	10/01/2018		
37	09/03/2016	77	27/04/2017	117	16/01/2018		
38	21/03/2016	78	03/05/2017	118	22/01/2018		
39	02/04/2016	79	09/05/2017	119	28/01/2018		
40	14/04/2016	80	15/05/2017	120	09/02/2018		

Table 2-1 List of the processed images. In yellow, the images that have been used in the STEP-2 of the processing.

Satellite	Sentinel-1
Acquisition mode	Wide Swath
Period	Jan 2015 - Apr 2018
Minimum revisit period [days]	6
Wavelength (λ) [cm]	5.55
Polarization	VV
Full resolution (azimuth/range) [m]	14/4
Multi-look 1x5 resolution (azimuth/range) [m]	14/20
Multi-look 2x10 resolution (azimuth/range) [m]	28/40
Orbit	Descending
Incidence angle of the area of interest	36.47° - 41.85°

Table 2-2 Dataset summary.

3 PROCEDURE DESCRIPTION

3.1 Deformation Activity Map

The S-1 data processing has been done by using software tools developed by CTTC in the framework of the European Project Safety. The used approach is based on the processing chain explained in Devan  ry et al., 2014, with the introduction of the coherence analysis. The main steps of the procedure are resumed in the flow chart of Figure 3-1. The first step (STEP 0) generates the interferograms and coherences, which will be used in the following steps for the estimation of the velocities and displacement time series over a subset of pixel (PS).

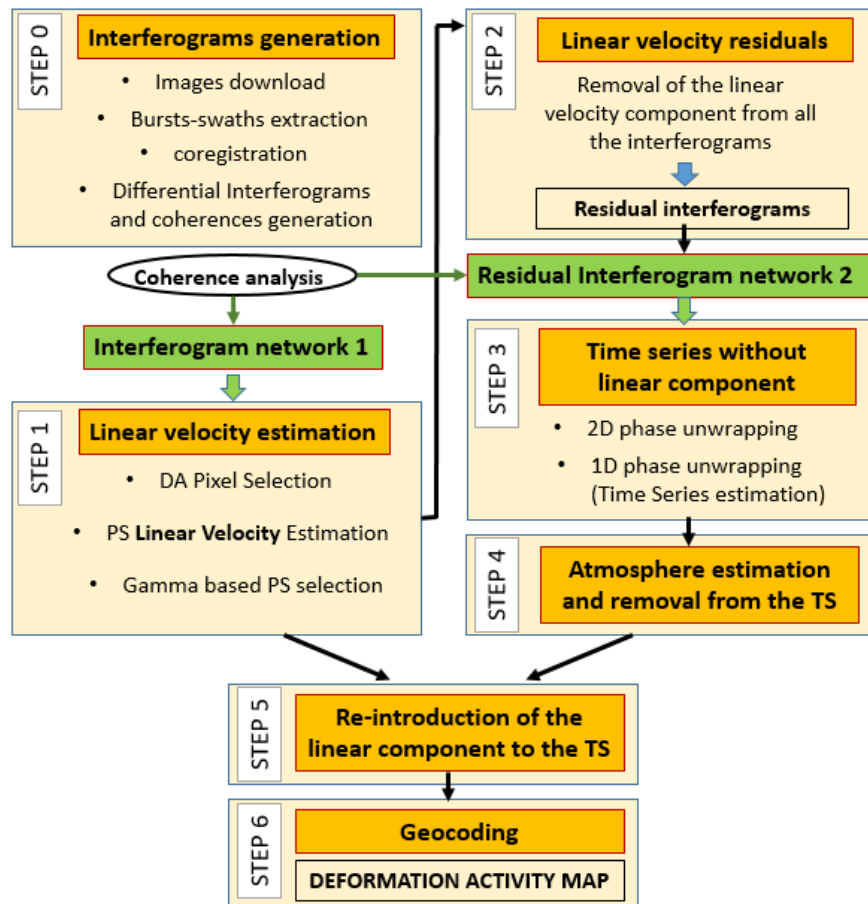


Figure 3-1: Flow chart of the data processing

Based on an analysis of the coherences, a first subset of interferograms has been selected to estimate the annual linear velocities over a subset of PS (STEP 1). Then, the phase component related to the estimated linear velocity is removed from the wrapped interferograms in order to:

- Reduce possible phase unwrapping errors in the STEP 3,
- Avoid estimating movement as part of the atmosphere component (see below).

The output of the STEP 2 are the interferometric phases of the selected pixels, without the linear component: we call them “residual interferograms”. Then, a second subset of interferograms is selected on the base of the coherence analysis. The residual interferograms are used in order to derive the time series (STEP 3) without the linear displacement component. The time series at this point represent mainly the atmosphere component (APS) and the non-linear component of the movements. The atmospheric component at each image is then estimated and removed from the TS (STEP 4). Then, the linear movement component is added again to the APS-cleaned TS in order to have the final deformation time series (without APS). Most of the steps are described in existing literature, e.g. Devanthery et al., 2014 and Barra et al., 2017. Here below are commented the key input parameters, the key steps and the main experienced difficulties.

3.1.1 STEP-0 Calculation of interferograms and coherences

The main steps are resumed in the first block of Image 3-1 and in the literature (Ferretti et al., 2017, part B). All the differential interferograms, together with the related coherences, with a maximum temporal baseline of 600 days have been generated. Based on these criteria, 4012 interferograms have been generated both full and 2x10 multilooked resolution (see Table 2-2). Depending on the processing approach, different subsets of interferograms will be used. In order to select the 2 interferogram groups, a criteria based on both the temporal baseline and the coherence analysis has been applied.

3.1.2 Coherence analysis

A new software tool has been developed with the aim of analyzing the behavior of coherence in time. The software calculates the mean coherence within a window (Figure 3-2), for all the interferograms. The window has been chosen with the aim of mainly represent the mountainous areas, where the coherence is more instable because affected by the seasonal changes and thus, where is more difficult to get PS results. One of the outputs is the so-called Coherence Matrix (Figure 3-3), it allows to easily visualize how the coherence change depending on both the temporal baseline and the period of the year. Coherence matrix is a symmetric diagram showing the calculated mean coherence values. Each x-y position indicates the master-slave acquisition dates of the related interferogram. The diagonal are the theoretical interferograms with temporal baseline (Δt) equal to zero. By moving away, in a symmetrical way, from the diagonal, the temporal baseline of the represented interferograms increases with steps of 6 days. The black zones means no-interferogram. The possible reasons for the absence of interferograms are: 1) the image is not available and 2) the interferogram has not been generated, e.g. because a maximum temporal baseline has been selected for the generation of the interferograms.

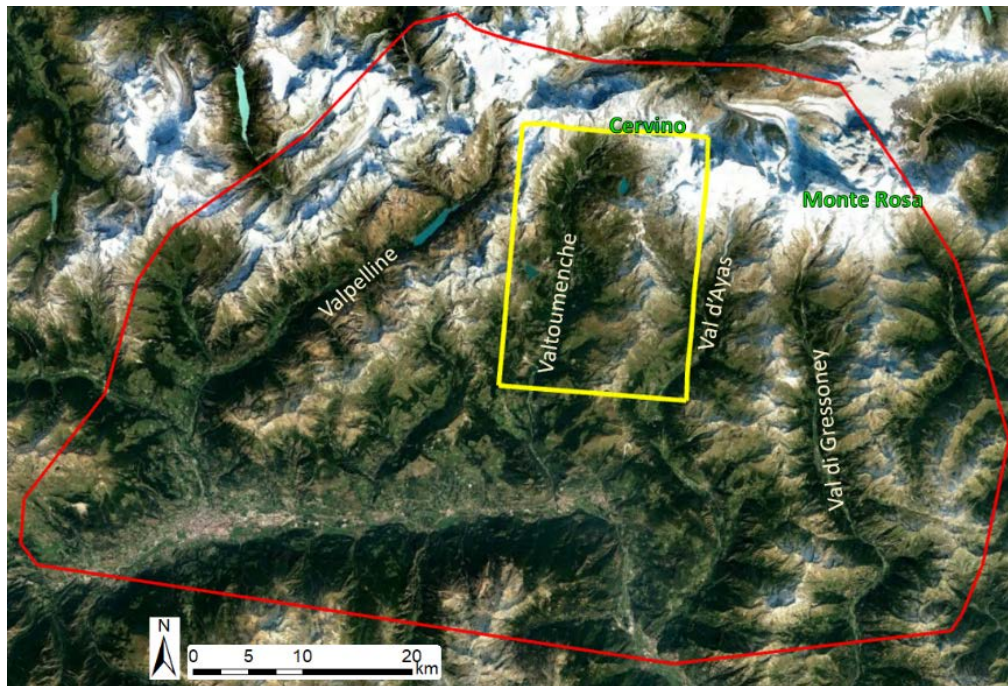


Figure 3-2: In yellow, the area used for the coherence analysis.

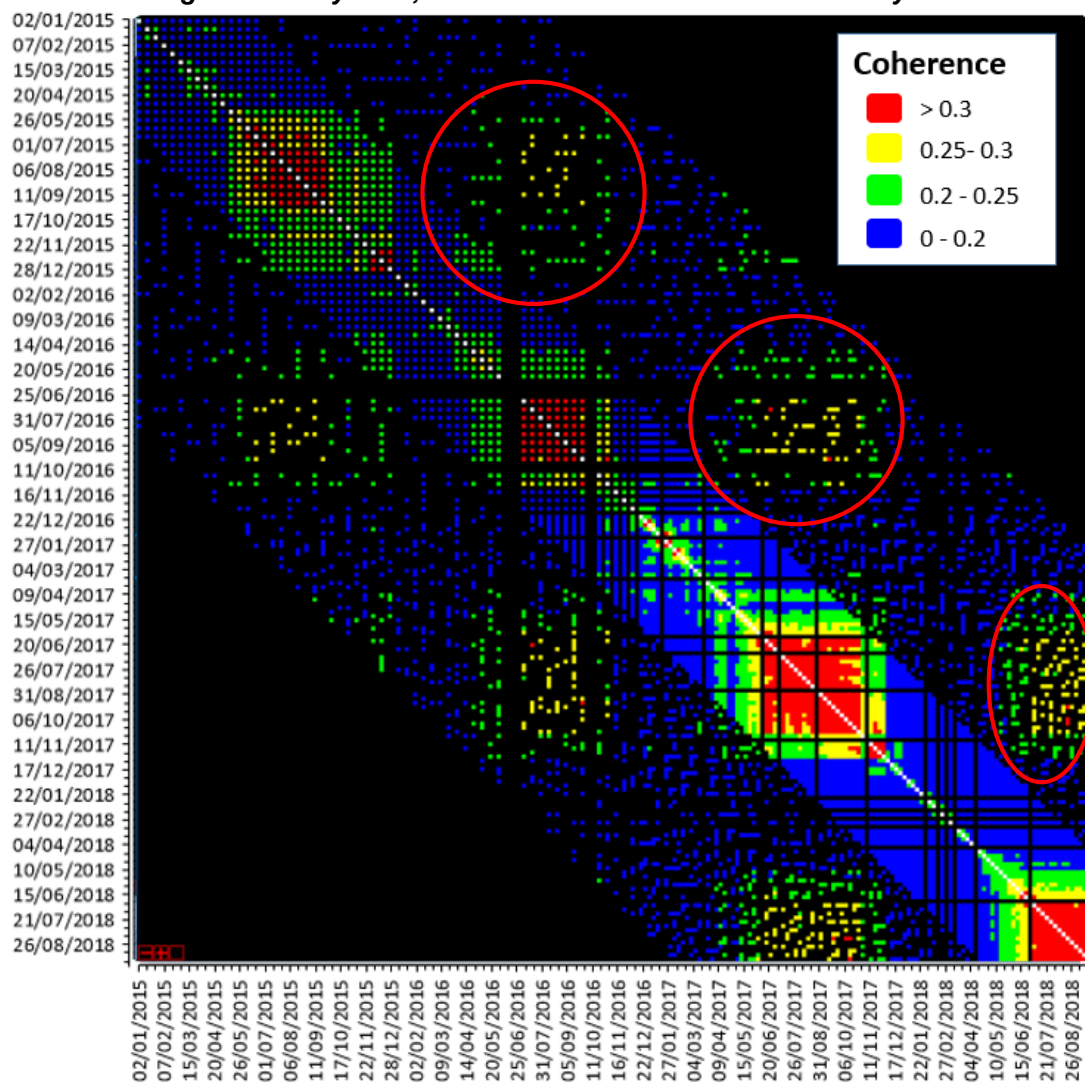


Figure 3-3: Flow chart of the data processing

Looking at the Coherence Matrix, you can observe:

1. The coherence of the area is generally low (rarely higher than 0.35).
2. We find the higher coherences in correspondence of few periods in a periodical way during the years. Specifically, we find the higher coherences in interferograms generated with two images acquired in warmer seasons (from May to November). On the contrary, you see a drastic drop off in the coherence during winters. Even the 6-days interferograms show very low values of coherence (<0.25) in the colder seasons. That means not only that the 6-days interferograms have higher coherence during summers, but also that we have interferograms with one-year temporal baseline that present higher coherences than others with lower Δt , if generated with two summer-images (highlighted by the red circles of Figure 3-3).
3. A drastic change in the continuity of the diagram colors, corresponding with the first acquisition of S-1B over the study area (28/12/2016), when we have an image every 6 days. Consequently, we have more interferograms.

3.1.3 STEP-1 Linear velocity estimation

The used methodology estimates the linear velocities, over selected pixels (PS), from a stack of wrapped interferograms. The interferogram network used for the velocity estimation has been selected on the base of both the temporal baseline and the coherence analysis. We have selected the interferograms with both a minimum Δt of 150 days and a minimum mean-coherence in the selected window (see previous chapter) of 0.2, i.e. the interferograms highlighted by the red circle of Figure 3-3. In this way, the interferogram network used for the estimation of the annual velocities is composed of 423 interferograms. Several statistical criteria are available to discriminate the noisier pixels from those with low level of noise (Crosetto et al., 2016). In Valle d'Aosta test site, the first selection of points has been based on the Dispersion of Amplitude (DA) (Hanssen, 2001). Over those points, the best-fitting linear model of velocity is estimated. Then, a second selection of points is performed based on a parameter (γ) quantifying the residuals between the model and the observations, i.e. the level of fitting between the linear model and the observations (interferograms). Since the deformation model is linear, restrictive γ threshold can cause the non-selection of the points with a strong non-linear movement. The general purpose of setting thresholds to select points is to find a good compromise between the quality of the selected points (low noise) and a good spatial coverage. Hence, for each case, different criteria are evaluated in order to find the best trade-off. In Valle d'Aosta low thresholds have been set in order to improve the number of points. The number of PS at the end of this step is 485.806.

<i>Minimum Temporal Baseline of the interferograms</i>	150
<i>Mean Coherence threshold</i>	0.2
<i>N of used interferograms</i>	423
<i>DA threshold</i>	0.4
<i>Gamma threshold</i>	0.84
<i>Final N of PS</i>	485.806
<i>Standard deviation of velocities</i>	3.91

Table 3.1.3 Resume of STEP-1.

3.1.4 STEP-2 Residual interferograms

As previously introduced, in the step-2 the proportional part of the linear component of the movement is removed from all the wrapped interferograms (in terms of phase difference proportional to the temporal baseline of each interferogram). This step is important for the successive phase unwrapping phase, but still more important for the estimation of the atmosphere component (see STEP-4, section 3.1.6).

3.1.5 STEP-3 Time Series (TS) estimation

The interferogram network has been selected on the base of both the temporal baseline and the coherence analysis, as in the previous step but with different thresholds. TS estimation is based on the spatial phase unwrapping of all the interferograms (2D phase unwrapping) and on the temporal one (1D phase unwrapping). In order to avoid phase unwrapping errors (aliasing), it is very important 1) a spatial continuous sampling (coverage of PS), given by good coherence and 2) an high temporal sampling with respect to the displacement rates, given by short temporal baselines 3) slow movement changes in space and time. The redundancy of the observations is also crucial in order to detect and correct possible aliasing, and thus for the estimation of the unknowns (phase values at each image). High redundancy of observations means at least 5 interferograms for each image. By the way, the quality of observations is the key element to prioritize, if possible, on the redundancy. For this reason, a selection of the interferograms (observations) based only on the temporal baseline is not a good approach. Looking at the coherence matrix (Figure 3-4) you can have an idea on which images (unknowns) can be estimated, thanks to acceptable observations (interferograms) in terms of a combination of quality (coherence) and number (redundancy). For that reason, the processed images have been reduced to 106, the ones highlighted in yellow in Table 2-1, mainly acquired in the warmer months. The used interferogram network is composed by 1325 interferograms. Lower temporal baselines (< 150), with a minimum coherence of 0.2, have been prioritized for the selection of the interferograms. Then a flexible temporal baseline has been introduced in order to improve the redundancy. Figure 3-4 represent the characteristics of the used interferogram network. Based on statistical checks of the Time Series estimations, the results are provided only in a subset of points. Over the 485.806 PS of the velocity estimation, the time series have been estimated for a subset of 412.300 PS.

3.1.6 STEP-4 APS estimation and removal

The atmospheric phase component removal is an important step in any wide-area PSI processing. Its goal is to correctly separate the APS from the deformation signal. For the APS estimation, a low pass filter is applied to remove the low frequencies associated with large spatial correlation phenomena. Since the main active phenomena of Valle d'Aosta affect wide areas (i.e. Deep-seated gravitational slope deformation), the low pass can filter also a percentage of those movements with a consequent underestimation of the related displacements. In order to avoid this underestimation, the linear component of the displacement have been previously removed. An APS component is estimated for each image and then removed from time series.

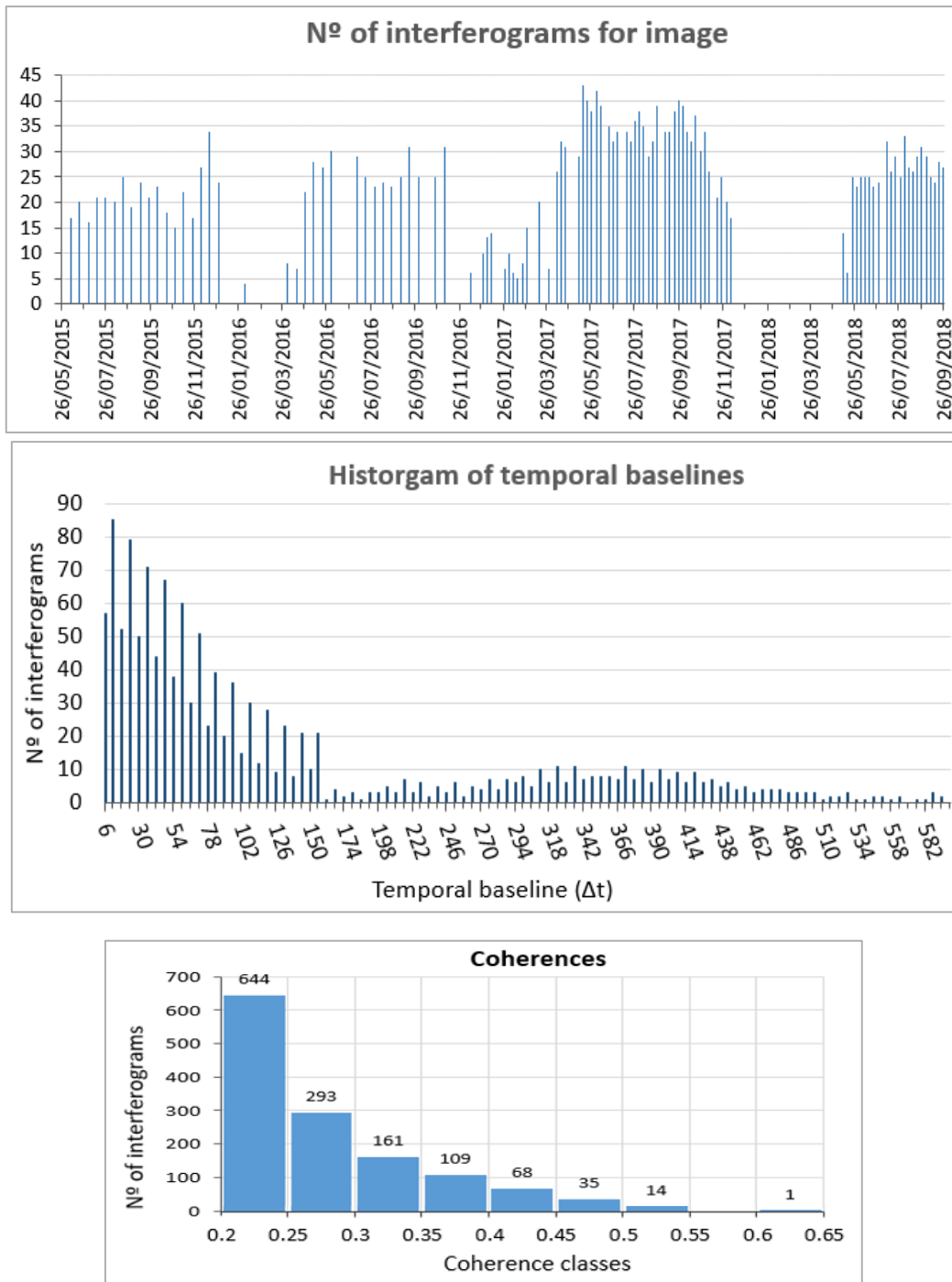


Figure 3-4: Resuming diagrams of the interferograms network used for the estimation of the Time Series. a) Representation of the redundancy of observations: the number of the interferograms for each image. b) Distribution of the temporal baselines. c) Distribution of the coherences.

Temporal Baseline of the interferograms	variable
Mean Coherence threshold	0.2
N of used interferograms	1325
Final N of PS with TS	412.300

Table 3.1.4 Resume of STEP-2.

3.1.7 STEP-5 Add linear component

Once we have the estimated time series without the atmospheric component, we re-introduce the proportional part of the linear movement component that was removed before, in order to have the final time series of LOS displacement.

3.1.8 STEP-6 Geocoding

This final step allow to pass from the radar geometry to the real one: at each point, corresponding to a line-column position in the radar image, a geographic coordinate is attributed. Moreover, all the information of the velocities and time series are put together in the same output, only the PS with both the information are maintained. This step allow to open the results in a GIS environment. The geocoding has been performed in WGS84 with the UTM, zone 32N, projection.

3.2 Active Deformation Areas Map and DAM

The Active Deformation Areas extraction is performed through the new software tool ADAfinder. ADAfinder is based on the algorithm developed in the framework of Safety and described in Barra et al, 2017, it has been developed in the framework of the European Project MOMIT (Navarro et al., 2018) and is following a continuous improvement based on its several applications (including U-Geahaz). The activity threshold used in order to extract the most significant active areas has been set as 2 times the standard deviation of the DAM velocity values ($2\sigma = 6,83 \text{ mm/yr}$). The influence radius of the points has been set to 26 m, while the minimum number of active neighborhood PS to be an ADA is 5. A total number of 434 ADA have been detected, between them 246 belong to the QI class 1 (reliable TS information), 76 to the QI class 2 (reliable, with some noise), 66 are classified as QI of 3 (to be checked) and 45 with a QI of 4 (not reliable). It is worth noting that the number of ADA is not representative of the number of active deformation phenomena, in fact the same phenomena can be represented by more than one ADA, depending on the coverage and spatial distribution of PS over the moving area.

The second output of ADAfinder is the final Deformation Activity Map (DAM) that is the result of a filtering of points based on criteria assessed in the framework of Safety and explained in Barra et al., 2017. The filtering is aimed at lowering the spatio-temporal noise of the DAM and improving the readability of the map.

DAM FINAL MAP	
DAM number of PS (velocities and TS)	400.013
DAM velocities standard deviation (σ)	3.42

Table 3-1 Resume of the final Deformation Activity Map.

4 MAP DESCRIPTION AND USE

Two maps have been delivered, in both shapefile format (.shp), representing the final versions of the DAM (point shapefile) and the ADA maps (polygon shapefile). The coordinate system for both shapefiles is WGS84, with the UTM projection, zone 32N, The ADA map represents the main goal of the task 2.3 “Landslides activity maps”. The DAM is the input for the generation of the ADA map, and is delivered for a more detailed level of information.

The DAM shape-file fields are resumed in Table 4-1, while ADA map shape-file fields are resumed in Table 4-2.

Field	Description	Units
<i>E</i>	WGS84 - UTM East	[m]
<i>N</i>	WGS84 - UTM North	[m]
<i>Lambda</i>	WGS84 Geographic Longitude	[°]
<i>Fi</i>	WGS84 Geographic Latitude	[°]
<i>ADA_ID</i>	ADA id. Containing the point [-1 if it is not part of any ADA]	
<i>Velocity</i>	Point displacement velocity	[mm/year]
<i>Def_mean</i>	Averaged deformation of the last 4 dates	[mm]
<i>Daaaammdd</i>	Deformation value at date aaaa/mm/dd	[mm]

Table 4-1 DAM field description.

Field	Description	Units
<i>ADA_ID</i>	Identity of the Active Deformation Area	-
<i>N_APS</i>	Number of point active point in the ADA	-
<i>X_MEAN</i>	UTM East	[m]
<i>Y_MEN</i>	UTM North	[m]
<i>VEL_MIN</i>	Minimum measured velocity	[mm/yr]
<i>VEL_MAX</i>	Maximum measured velocity	[mm/yr]
<i>VEL_CLASS</i>	Class of de ADA	1 if <i>VEL_MAX</i> > 10 mm/yr; 0 otherwise
<i>DEF_MEAN</i>	Averaged deformation of the last 4 dates	[mm]
<i>TNI_CLASS</i>	Temporal noise index	-
<i>SNI_CLASS</i>	Spatial Noise Index	-
<i>QI_CLASS</i>	Quality index	-

Table 4-2 ADA field description.

Figure 4-1 shows the DAM in terms of LOS velocities and Figure 4-2 the extracted ADA, through the parameters explained in the chapter 3.2, classified on the bases of the QI.

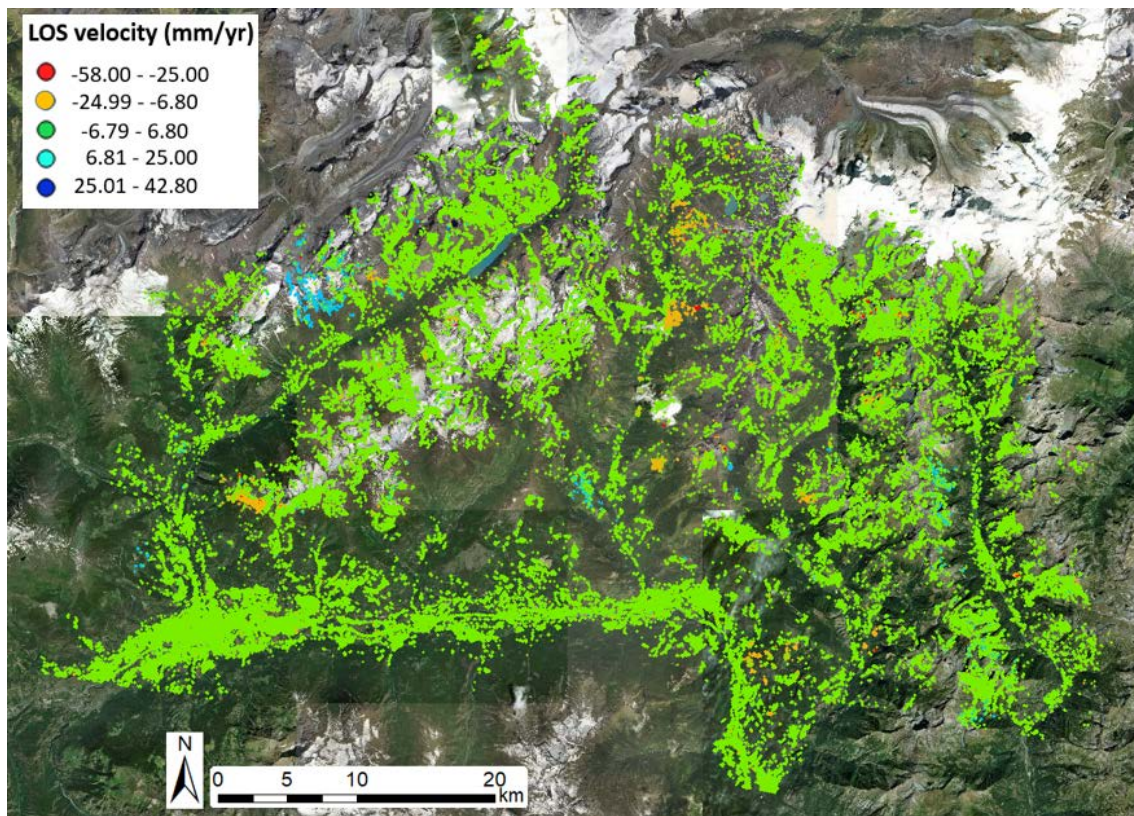


Figure 4-1: Deformation Activity Map (DAM).

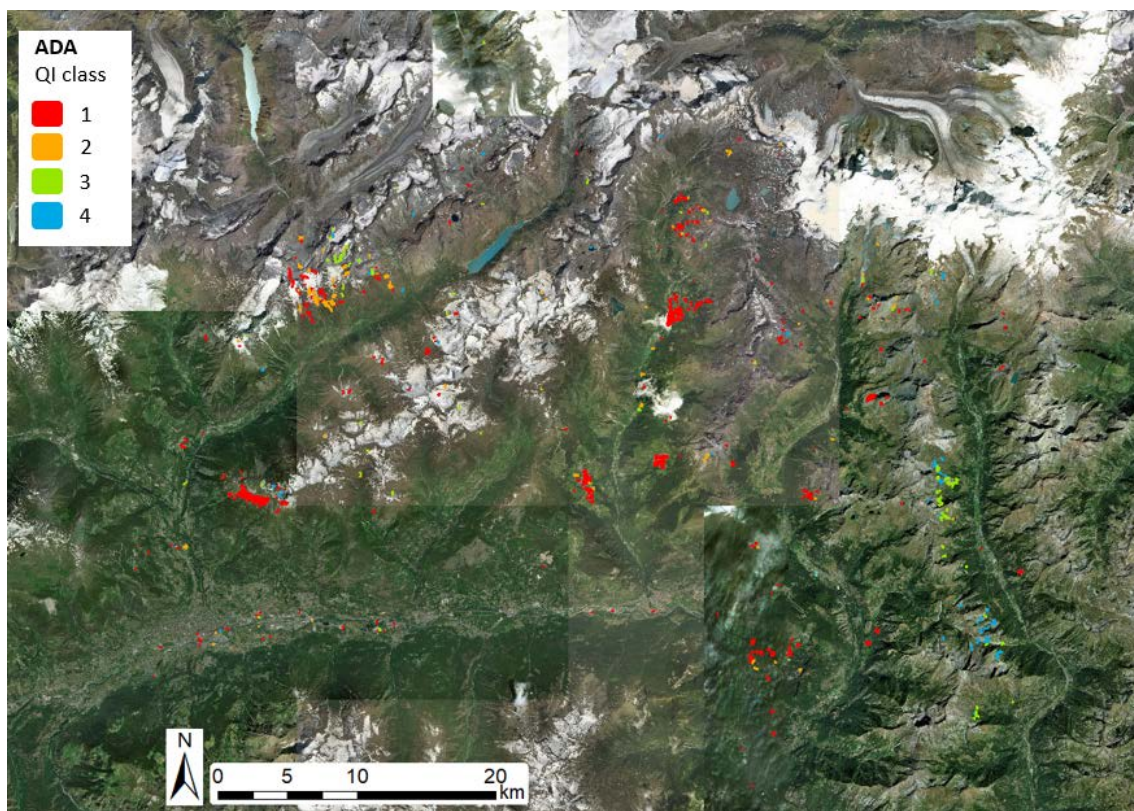


Figure 4-2: The extracted ADA, with at least 5 PS and the activity thresholds of 6,83 mm/yr (2σ). The colours represent the Quality Index classes.

4.1 DAM Time series

Figure 4-4 shows an example TS of two ADA relative to the same deformation phenomena. The first image of the figure shows the location of the analyzed ADA in the area of study. In the yellow square, a detailed view of the extracted ADA. Below, the median deformation TS of the PS within the 2 ADA. The error bars represent the standard deviation of the deformation values: in the example, in correspondence of January 2017 there is a strong peak of standard deviation (σ), meaning spatial noisy information. The gradual growth in the σ values of the active PS is intrinsically caused by the increasing of the accumulated deformation. The same graphic shows the temporal acquisitions of the processed images, i.e. the temporal sampling of the TS.

5 OBSERVATIONS

The Valle d'Aosta area presents some challenging aspects for what concerns the processing approach to be used in order to increase both the quality and the coverage of the results, mostly in the mountainous areas.

5.1 Improvements

- A different processing approach, including the coherence analysis for the selection of the interferogram networks, has been proposed with good results in terms of PS coverage.
- The coverage of PS has been improved (from 161.362 to 400.310), especially in the critical zones at higher altitudes.
- The coverage of PS with TS estimation has been strongly improved (from 105.397 to 400.310), also in the mountainous critical zones (higher altitudes).

5.2 Map interpretation notes

- Some effects of the atmosphere are still present.
- **Time series:** The estimated TS are slightly affected by atmosphere in some areas. Some aliasing are still presents in the TS.
- **ADA:** 434 active areas have been extracted. Many groups of ADA belong to the same deformation phenomena. The QI equal to 4 or 3 represents points that are strongly affected by atmosphere and spatial noise: the information is not reliable or need to be analysed.
- All the deformations TS and velocities are in **Line of Sight**, i.e. they represent the projection of the real 3D displacement in the direction "satellite-point".
- The positive values represent points that are going far from the satellite. The negative ones represent those, which are moving towards the satellite.
- We suggest to use the activity thresholds of 2 σ (6.8 mm/yr) for the visualization of the delivered velocity map (as presented in Figures 4-1 and 4-2). In this way, you visualize only the most reliable deformation without losing PS velocity information in correspondence of deformation phenomena. For a local, detailed, visualization you can change the colour scale.

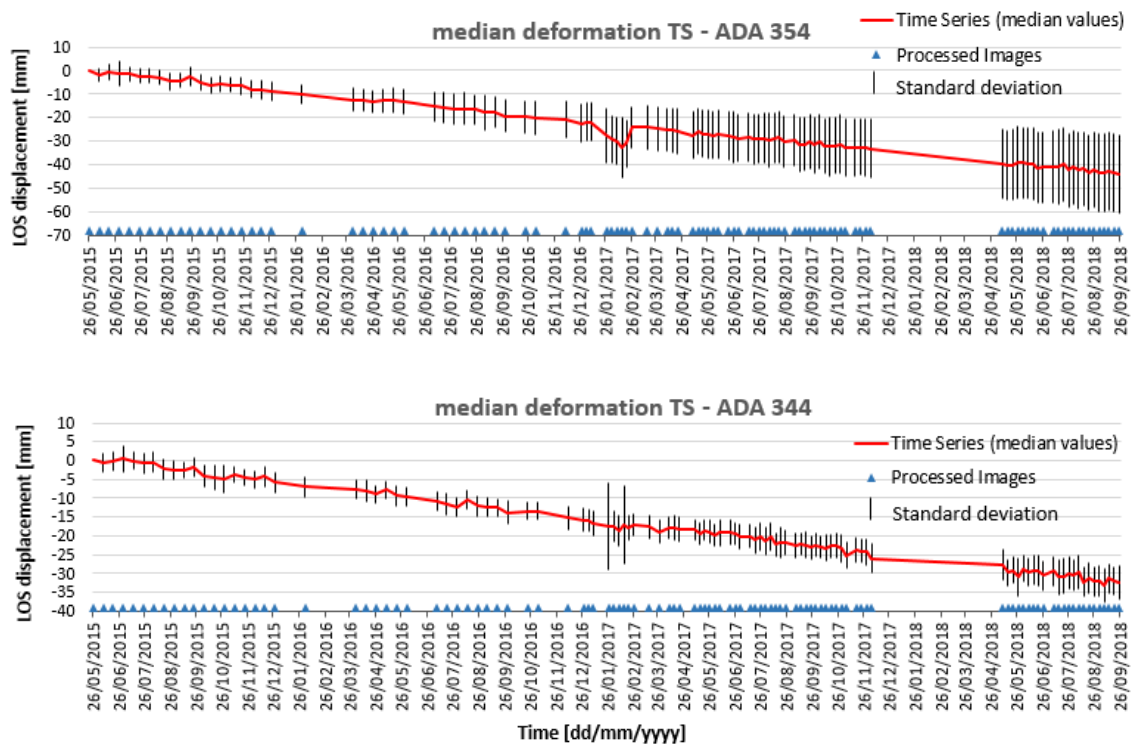
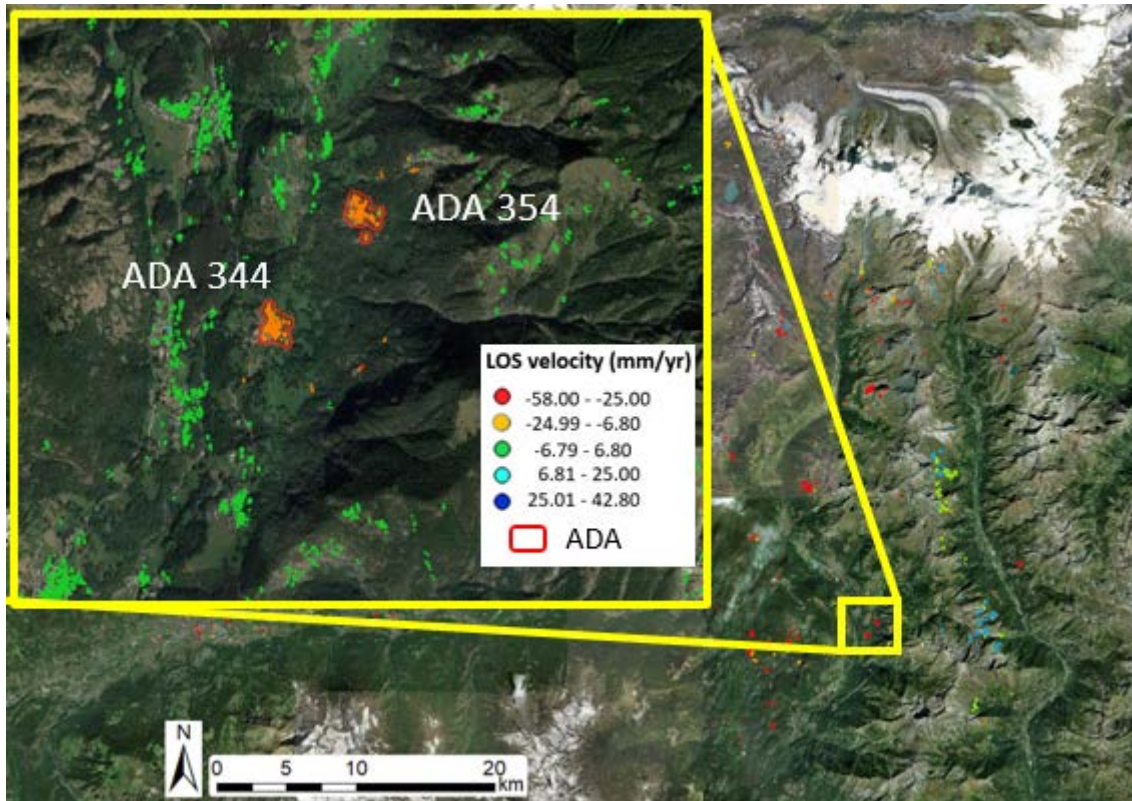


Figure 4-1: Example of TSs of 2 ADA ($QI=1$) probably belonging to the same deformation.

6 REFERENCES

- Barra, A., Solari, L., Béjar-Pizarro, M., Monserrat, O., Bianchini, S., Herrera, G. et al. (2017). A Methodology to Detect and Update Active Deformation Areas Based on Sentinel-1 SAR Images. *Remote Sensing*, 9(10), 1002.
- Cignetti, M., Manconi, A., Manunta, M., Giordan, D., De Luca, C., Allasia, P., & Ardizzone, F. (2016). Taking advantage of the esa G-pod service to study ground deformation processes in high mountain areas: A valle d'aosta case study, northern italy. *Remote Sensing*, 8(10), 852
- Crosetto, M., Monserrat, O., Cuevas-González, M., Devanthery, N., & Crippa, B. (2016). Persistent scatterer interferometry: a review. *ISPRS Journal of Photogrammetry and Remote Sensing*, 115, 78-89
- Devanthery, M. Crosetto, O. Monserrat, M. Cuevas-González, B. Crippa . An approach to persistent scatterer interferometry *Remote Sens.*, 6 (7) (2014), pp. 6662–6679.
- Ferretti, A., Monti-Guarnieri, A., Prati, C., Rocca, F., & Massonet, D. (2007). *InSAR Principles-Guidelines for SAR Interferometry Processing and Interpretation*, TM-19. The Netherlands: ESA Publications.
- Hanssen, R. *Radar Interferometry*. Kluwer Academic Publishers, Dordrecht, The Netherlands, 2001.
- Navarro, J. A., Cuevas-González, M., Barra, A., & Crosetto, M. Detection of Active Deformation Areas based on Sentinel-1 imagery: an efficient, fast and flexible implementation.